Yang *et al.*
European Journal of Medical Research (2025) 30:163
https://doi.org/10.1186/s40001-025-02360-6

European Journal of Medical Research

RESEARCH

Open Access

Identification of TAP2 as a novel immune target in human cancers: insights from integrated bioinformatics and experimental approaches

Lufei Yang[1,2,3,4†], Jiawei Gui[2,3,4,5†], Yilei Sheng[2,3,4,5†], Junzhe Liu[1,2,3,4], Chong Wang[1,2,3,4], Zhansheng Fang[1,2,3,4], Le Huang[2,3,4,5], Zewei Tu[1,2,3,4*], Xingen Zhu[1,2,3,4*] and Kai Huang[1,2,3,4,6*]

Abstract

Background Transporter 2, ATP binding cassette (ABC) subfamily B member (TAP2), encodes a protein within the ABC transporter superfamily. TAP2 plays a role in the progression of cancers, such as cervical, breast, and lung cancers. However, the relationship between TAP2 and cancer prognosis, immune cell infiltration, tumor microenvironment, and immunotherapy remains unexplored. Therefore, this study aims to investigate the effect of TAP2 expression on its role in predicting tumor prognosis and immunotherapy efficacy.

Methods Bioinformatics analyses such as Gene Set Enrichment Analysis, single-cell, and Connectivity Map analyses were used to comprehensively assess TAP2-related genomic alterations, prognostic value, enrichment pathways, single-cell expression patterns, and potential targeting inhibitors. In addition, molecular docking techniques were used to simulate drug binding to TAP2. WB and RT-qPCR were used to detect differences in TAP2 expression in glioma cell lines. The U251MG cell line was established with TAP2 overexpression. The effects of elevated TAP2 expression on GBM cell function was evaluated using various assays, including the Transwell migration, scratch, and clonal formation assays.

Results TAP2 exhibited aberrantly expression in tumor tissues with genomic alterations. TAP2 significantly correlates with poor prognosis across various cancers. It was also involved in immune-related pathways, immune infiltration, and immune checkpoint regulation, thereby influencing the tumor microenvironment and immune response to cancer. TAP2 was identified as a potential predictor of immunotherapy response and screened for potential targeted inhibitors for future therapeutic interventions.

Conclusions Our findings suggest that TAP2 may serve as a promising prognostic marker and immune target in human cancers, warranting further investigation into its role in tumor immunity.

Keywords Immunotherapy response, Molecular docking, Pan-cancer, Prognostic biomarker, TAP2

†Lufei Yang, Jiawei Gui and Yilei Sheng contribute equally to this work.

*Correspondence:
Zewei Tu
tuzewei@email.ncu.edu.cn
Xingen Zhu
ndefy89006@ncu.edu.cn; kaihuang@ncu.edu.cn
Kai Huang
kaihuang@ncu.edu.cn
Full list of author information is available at the end of the article

Introduction

Cancer has emerged as a major social and public health challenge of the twenty-first century, accounting for approximately a quarter of deaths from noncommunicable diseases [1]. As the global population continues to grow and age, cancer rates rise significantly worldwide [2, 3]. Therefore, actively exploring novel methods and targets for cancer treatment is essential for improving public health [4]. With advancements in cancer treatment, immunotherapy has become a key approach for numerous tumors [5, 6]. Extensive research on tumor resistance and immune escape significantly contributes to the advancement of cancer immunotherapy [7–9].

CD8 + T cell-mediated cytotoxicity is a crucial pathway in immune response. CD8 + T cells are activated when T cell receptors interact with peptide-major histocompatibility complex class I, leading to the release of cytotoxic molecules through the immune synaptic perforin membrane, which mediates tumor cell death [10, 11]. Therefore, the expression level of MHC-I molecules with tumor antigen peptides in tumor cells primarily determines the ability of cytotoxic T lymphocytes to eliminate tumor cells.

Transporter 2, member B of the ATP-binding cassette (ABC) subfamily (TAP2) (also known as APT2, PSF2, or ABC18), is a protein encoded in the human genome and belongs to the ABC transporter superfamily. TAP2 combines with transporter 1, ABC subfamily B member (TAP1) protein, to form a functional heterodimer complex known as the transporter associated with antigen processing (TAP) protein on the endoplasmic reticulum (ER). This complex is a crucial component of the peptide-loading complex in the ER [12]. TAP is responsible for loading high-affinity peptides onto MHC-I, which are then transported to the cell surface for presentation to CD8 + T cells. Emerging evidence suggests that dysregulation of the TAP complex significantly affects the immune response by facilitating atypical cross-presentation and enhancing T cell activation. The blockade of TAP activity disrupts the canonical MHC-I antigen presentation pathway to CD8 + T cells, potentially impairing the ability of the immune system to detect and eliminate infected or transformed cells [13]. The expression of TAP2 strongly correlates with survival rates in various cancer types, such as cervical, breast, and lung cancer [14–17]. A study shows that mutated TAP2 affects MHC-I function [18], while the overexpression of TAP2 enhances antitumor drug resistance of human cancer cells [19]. These findings indicate the pivotal role of TAP2 in immune recognition and highlight its potential as a prognostic biomarker and therapeutic target in oncology. However, its effect on predicting tumor immune invasion and immunotherapy response remains unclear, and no comprehensive pan-cancer studies on TAP2 exist to date.

TAP is not only associated with various types of cancer but also implicated in a spectrum of autoimmune diseases [20–22]. Research has demonstrated that the differential expression of TAP could significantly affect the therapeutic outcomes of combined radiotherapy and immunotherapy [23]. In our prior studies, we identified TAP1, a component of the TAP heterodimer, as a robust predictor of prognosis in cancer immunotherapy [24]. Concurrently, we also discerned the potential of TAP2 to serve as both a therapeutic target and a prognostic indicator in cancer immunotherapy. To elucidate this aspect, our study aims to elucidate the influence of TAP2 expression on malignant behavior in a glioma cell line, while analyzing its role in predicting tumor prognosis and immunotherapy efficacy.

Methods

A comprehensive flowchart delineating the foundational concepts of this study is presented in Fig. 1.

Gene and protein expression analysis

The TCGA Pan-Cancer Cohort and Genotype-Tissue Expression (GTEx) dataset, which includes mRNA expression level data from tissue samples along with clinical information about the source patients, was downloaded from the UCSC Xena database (https://xenabrowser.net/datapages/). Differential expression genes (DEGs) in the TCGA database were identified based on TAP2 expression levels using the "limma" package in R software. The cBioPortal web tool (http://cbioportal.org) was used to analyze the frequency of TAP2 genome alternations across various tumors [25]. Transcriptome data for 21 cancer cell lines was obtained from the Cancer Cell Line Encyclopedia (CCLE: https://sites.broadinstitute.org/ccle/) website is used to obtain [26]. The distribution of TAP2 Protein at the subcellular level was obtained from the Human Protein Atlas (HPA: https://www.proteinatlas.org/) database, while the protein interaction analysis results were sourced from the compartmentalized Protein–Protein interaction database (ComPPI: http://comppi.linkgroup.hu) [27].

Survival and prognosis analysis

Kaplan–Meier (K–M) curve and Univariate Cox regression were used to analyze the correlation between patient prognosis in multiple tumors and variations in TAP2 expression levels in tumor cells. The types of prognostic data included disease-free interval (DFI), overall survival (OS), progression-free interval (PFI), and disease-specific survival (DSS). These data were obtained from the UCSC Xena database (https://xenabrowser.net/datapages/).

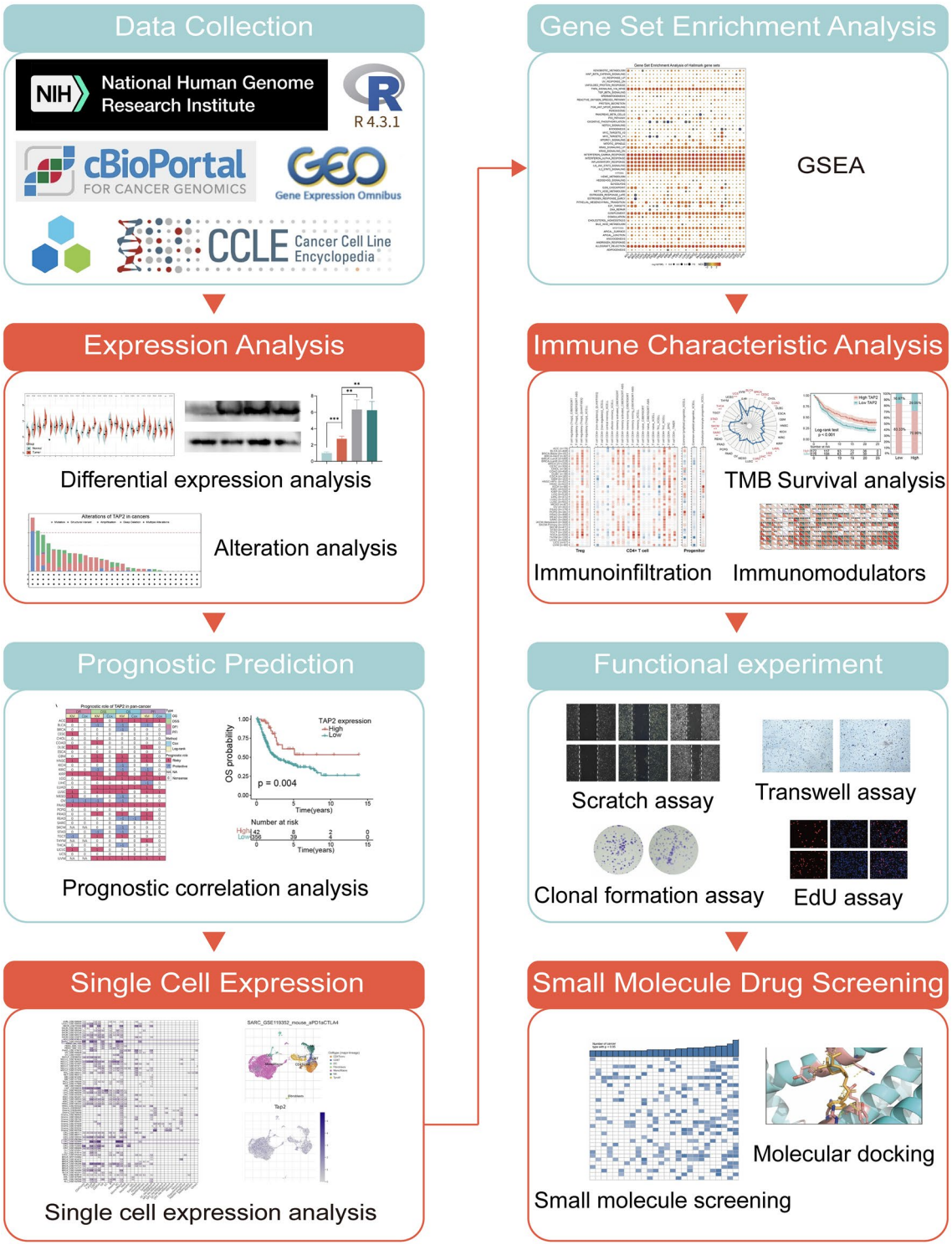

Fig. 1 The comprehensive process of the basic methods of this study

Subsequently, the R package "Survminer" in R software was used to calculate the log-rank P-value, 95% confidence interval (CI), and hazard ratio (HR) from the K-M method and univariate survival analysis, visualizing the results.

Single cell expression and gene set enrichment analysis

The Tumor Immune Single-cell Hub 2 (TISCH2) web tool (http://tisch.comp-genomics.org/home/) was used for single-cell expression analysis. The analysis parameters include TAP2 (Gene), major lineage (Cell-type annotation), and all cancers (Cancer type). The analysis results were presented using heat maps, scatter plots, and violin plots. Gene set enrichment analysis was performed using datasets from the Molecular Signatures Database website (MSigDB, https://www.gseamsigdb.org/gsea/index.jsp), specifically the "GMT" file of the hallmark gene set (h. all. V7.4. Symbols. GMT), which included 50 marker genes. Based on these data, the normalized enrichment score and false discovery rate of DEGs between tumor groups with varying TAP2 expression across multiple cancer types were calculated, while a GESA analysis was performed using the R package "clusterProfiler" [28] in the R software.

Immune infiltration and immunotherapy prediction analysis

The public database Tumor Immune Estimation Resource 2.0 (TIMER2 http://timer.cistrome.org/) was employed to investigate the relationship between TAP2 and Immune cell infiltration levels [29]. The analysis included 21 types of immune cells: eosinophil, B cells, cancer-associated fibroblasts, common lymphoid progenitors, myeloid progenitors, granulocyte-monocyte progenitors, myeloid-derived suppressor cells, dendritic cells, endothelial cells (Endo), hematopoietic stem cells (HSCs), CD4 + T cells, neutrophils, γ/d T cells, Natural killer cells (NK), Endo, HSCs, NK T cell, T cell follicular helper (Tfh), macrophages, monocytes, CD8 + T cells, mast cells, and regulatory T cells. Spearman correlation analysis was performed on some well-known immune-related factors and TAP2 expression using the downloaded data. In addition, a statistical correlation was calculated between TAP2 and immunomodulators across various tumor types using Spearman correlation analysis. Tumor mutation burden (TMB) and microsatellite instability (MSI) scores were obtained from the TCGA. Visualization of analytical data was performed using the R package "ggradar." Additionally, prognostic data (including OS and PFS) were obtained from two immune checkpoint-blocking treatment cohorts to assess the potential of TAP2 to predict the susceptibility of patients to immunotherapy. Patients (n = 288) with urological cancer were treated with atezolizumab (anti-PDL1) in the IMvigor210 cohort, while patients (n = 51) with melanoma were treated with nivolumab (anti-PD1) in the GSE91061 cohort. Survival analysis was performed and visualized using the R package "Survminer."

Plasmid transfection and cell cultivation

SVG P12, SW1088, U251MG and T98G cell lines were cultured for western blot and RT-qPCR assays. The SW1088 cell lines were purchased from ATCC cell bank, while the remaining cell lines were purchased from Culture Collection of the Chinese Academy of Sciences (Shanghai, China). The functional experiments were conducted using the U251MG cell line. All cell lines—except for the SW1088 cell line, which was cultured in L-15 complete culture medium—were cultured in DMEM medium (Thermo Fisher, American) supplemented with 10% fetal bovine serum (Thermo Fisher, American) and 1% streptomycin-penicillin solution (Thermo Fisher, American) in a 37℃ incubator with 5% CO2 [30]. The TAP2 gene fragment was amplified from the cDNA of the U251MG cell line via PCR and then cloned into the p3xFLAG-CMV-7.1 vector using the restriction enzymes EcoRI and XbaI. Primers are as follows: F, ATGCGGCTCCCTGACCTG; R, TCAGTCCAT CAGCCGCTG [17]. The U251MG cell line was subjected to plasmid transfection. Before plasmid transfection, all cells were inoculated in 6 cm culture dishes and grown to the logarithmic phase. The plasmid mixture was prepared according to the plasmid requirement of 3 μg per dish using Opti-MEM (Thermo Fisher, American), with Lipo3000 and P3000 (Thermo Fisher, American) as transfection reagents. The culture medium was replaced 6 h after transfection.

Western blotting and RT-qPCR

Protein samples were extracted and homogenized with lysis buffer (Solarbio, China). The mixture was then centrifuged at 4℃ for 10 min using a high-speed refrigerated centrifuge, and the supernatant was obtained from the centrifuge tube. The extracted total protein samples were mixed with a quarter volume of Sodium dodecyl sulfate (SDS) loading buffer (Solarbio, China) and heated at 100 ℃ for 10 min. The heated protein samples were then loaded onto an SDS-PAGE gel alongside a protein marker (MSDS P6110 Triple Color Prestained Protein Ladder, Uelandy, China). Subsequently, Polyvinylidene fluoride (PVDF) membranes with a pore size of 0.22 μm were used to transfer the proteins. The transferred PVDF membrane was sealed with 10% milk for 2 h and then rinsed three times with TBST diluent. The bands were incubated overnight at 4 ℃ with anti-TAP2 (1:1000, 10161-1-AP, Proteintech, China), anti-Flag tag (1:20000, 20543-1-AP, Proteintech, China) and anti-GAPDH (1:5000, 10494-1-AP, Proteintech, China), respectively. After rinsing, the PVDF membrane was co-incubated with the secondary antibody, followed by luminescence imaging using the developer [31].

A total RNA extraction kit (Bioflux) was used to extract RNA. After calculating the concentration, 1 μg of the extracted total RNA was reverse transcribed into the cDNA of the corresponding sample using a reverse transcription kit. After obtaining cDNA, a suitable system was prepared using SYBR Green fluorescent quantitative PCR enzyme (Yeasen, China), to which equal amounts of cDNA diluent and TAP2 or GAPDH primers were added. The experimental results are presented by histogram. Primers used in this experiment are: TAP2-F, CCCTGG CCGAGCGTA; TAP2-R, AAATCCCAGCAGCCCTCT TAG; GAPDH-F, TATGAGAGCTGGGGAATGGGA; GAPDH-R, ATGGCATGGACTGTGGTCTG.

Wound healing and transwell migration assay

Five evenly spaced horizontal lines were drawn on the back of the six-well plate using a ruler and marker. U251MG cell lines treated as controls and U251MG cells transfected with the TAP2 overexpression plasmid were cultured to the logarithmic growth phase. The cells were digested with trypsin, and a cell suspension of 4×10^4 cells/ml was prepared using a medium containing 10% serum. The cell suspension was added to each well of the six-well plate at a density of 1×10^5 cells per well, and then the culture dish was gently shaken to ensure even cell distribution. When the cell confluence reached approximately 70%, a vertical line was drawn across the bottom of the culture dish using a 200 μL pipette tip. After drawing the line, the medium was immediately replaced with a 2% low-serum medium, and the scratch was recorded as 0 h under the microscope. The photos were captured again at 24 h and 48 h [32]. The control U251MG cells and U251MG cells statically transfected with the TAP2 overexpression plasmid were cultured until they reached the logarithmic growth phase. The cells were digested with pancreatic enzyme, and digestion was terminated using 10% serum medium to prepare a 4×10^4 cells/ml suspension. The Transwell chamber (Corning, American) was placed in a 24-well plate (Corning, American), with 2×10^4 cells per well. A 2% low-serum medium was added to the upper layer of the Transwell chamber, while a 10% fetal bovine serum medium was added to the lower layer, ensuring that the medium did not penetrate the bottom membrane of the chamber. It was cultured for 3 days in a 37℃ incubator with 5% CO_2. After removing the medium, the cells were fixed with 4% paraformaldehyde, while gentian violet dye was applied for staining. After rinsing, the cells were photographed at 200× magnification to observe cell migration [33, 34].

EdU labeling to assess cell proliferation

The control U251MG cells and U251MG cells statically transfected with TAP2 overexpression plasmid were cultured to the logarithmic growth phase, digested with trypsin, and the digestion was terminated with 10% serum medium to prepare a 4×10^4 cells/ml suspension. The cells were inoculated in a 12-well plate at a density of 1×10^5 cells per well. After 24 h of attachment, an EdU (5-ethynyl-2'-deoxyuridine) working solution (Beyotime, China) was prepared according to the manufacturer's instructions, added to the medium, and incubated in the dark for 2 h. The medium was then discarded, and the cells were rinsed three times with a washing solution. Hoechst dye (Beyotime, China) was added to each well and incubated for 10 min in the dark, followed by three rinses with washing solution. Fluorescently stained cells were photographed under a fluorescence microscope [34].

Clonal formation experiment

The negative control U251MG cells and U251MG cells stably transfected with TAP2 overexpression plasmid were cultured to the logarithmic growth phase. The cells were then digested with trypsin, and the digestion was terminated with a 10% serum medium. A 150 cells/ml suspension was prepared. The cell suspension was added to a six-well plate at a concentration of 300 cells per well, and the cells were evenly distributed by gently shaking the plate. The cells were cultured for 10 days at 37 ℃ in a 5% CO_2 incubator. The cells were fixed with 4% paraformaldehyde after removing the medium, stained with gentian violet dye, washed, and photographed to capture monoclonal growth [17].

Screening of potential targeted small molecule inhibitors

To identify upregulated and downregulated genes, we categorized DEGs between low and high TAP2 subgroups based on their log2-fold changes. Subsequently, the Connectivity Map (CMap) database was employed to identify small molecules with expression patterns that were opposite to those of TAP2. Small molecule inhibitors were selected based on a CMap score (score < -50), where a negative score indicates their potential to target TAP2. Subsequently, AutoDock Vina 1.2.2 was employed to assess the binding energy and interaction modes between the identified small molecules and TAP2 [35]. The 3D structure of the TAP2 protein was retrieved from the Protein Data Bank (PDB: 5U1D) and processed using PyMOL2.5. The 3D structures of the small molecules were sourced from the PubChem database (https://pubchem.ncbi.nlm.nih.gov/). After the molecular docking process was completed, the resulting 3D models were visualized using PyMOL2.5.

Statistical analysis

The Wilcoxon rank sum test was used to analyze the statistical significance of the differences in TAP2 expression between normal and tumor tissues. TAP2-related survival and prognosis were evaluated using univariate Cox regression analysis, K–M method, and log-rank test. Spearman's correlation analysis was conducted to assess the correlation between several other factors and TAP2. In cancer subgroups with differential TAP2 expression, we calculated the statistical significance of the proportion of immune checkpoint inhibitor (ICI) responders and nonresponders. Image processing was conducted using ImageJ software. The results of the experiments were statistically analyzed using GraphPad Prism 8.0. The two groups were compared using an unpaired t-test. A p-value of < 0.05 indicated statistical significance, with the * ($p < 0.05$), * * ($0.05 < p < 0.001$), * * * ($p < 0.001$). All experiments were repeated three times.

Results

Differential expression analysis and alteration of TAP2

Firstly, TAP2 expression levels in various cancers and normal tissues were analyzed and compared using data from the TCGA and GTEx databases. Additionally, high expression of TAP2 was observed in the following TCGA cancers: BLCA, CESC, CHOL, COAD, ESCA, GBM, HNSC, KIRC, KIRP, LAML, LGG, LIHC, PAAD, READ, SKCM, STAD, and TGCT. However, low TAP2 expression was observed in some cancers, including ACC, BRCA, KICH, LUAD, OV, PRAD, and THCA. In LUSC and UCEC, normal tissues exhibited similar levels of TAP2 expression (Fig. 2A). The comparison showed that TAP2 mRNA expression in GBM was significantly higher than in normal tissues (Fig. 2B).

To validate this conclusion, the protein expression of TAP2 was assessed in astrocyte and glioma cell lines using western blotting (Fig. 2C), and mRNA expression was measured in the same samples using RT-qPCR (Fig. 2D). The results showed that TAP2 expression was significantly increased in gliomas, consistent with previous analysis results, suggesting that TAP2 may influence the malignancy of gliomas.

Subsequently, the database was used to investigate TAP2 genomic alterations across pan-cancer. Although the alteration rate of TAP2 was low in all tumors, diffuse large B-cell lymphoma (DLBC) exhibited the highest frequency of alterations, with over 8% of patients with DLBC showing TAP2 deep deletions, affecting approximately two-thirds of these cases (Fig. 2E). To investigate the potential association between high TAP2 and its copy number variations (CNV), a correlation analysis of TAP2 expression and alteration was conducted across 33 cancer types. The results showed that high TAP2 expression was associated with mutations in some tumors, with the strongest correlation observed in KLHC (Fig. 2E). Furthermore, regression analysis was performed on TAP2 expression levels and its CNV in KLHC, revealing a positive correlation between the two (Fig. 2F, $p = 0.01$). Combined with the previous analysis results, the lower expression of TAP2 in KIHC compared with normal tissues may be attributed to the low alteration rate.

Immunofluorescence images showed that the TAP2 protein was predominantly localized in the nuclei and ER of A-431 and U251MG tumor cells (Fig. 2G). Finally, to construct the protein–protein interaction (PPI) network, the comPPI interaction data was employed. The image depicted the distribution of TAP2-related proteins primarily in the cytosol, extracellular, membrane, mitochondrion, nucleus, and secretory pathway (Fig. 2H).

Prognostic role of TAP2 plays in pan-cancer

OS refers to the duration from treatment initiation to death and serves as a key standard for survival analysis in most cancers. However, it often contains the potential for death from causes unrelated to tumors. To comprehensively evaluate the effect of TAP2 on the prognosis of various tumors, the role of TAP2 was analyzed in pan-cancer prognosis using OS, DSS, DFI, and PFI and generated a heatmap (Fig. 3A). Results showed that TAP2 expression was associated with an increased risk in all analyzed cancer types except for CHOL, ESCA, PCPG, SARC, and UCS. In certain cancers, such as OV, TAP2 may act as a protective factor. The outcome of PAAD suggests that TAP2 expression is associated with a poor prognosis across all indicators.

The correlation between TAP2 expression and the prognosis of 32 patients with TCGA was further analyzed using univariate Cox regression, with the results illustrated in a forest plot. The forest plot indicates that reduced OS time was significantly associated with high TAP2 expression levels in LUAD (HR = 1.268 [95% CI, 1.089–1.476], $p = 0.002$), ACC (HR = 1.470 [95% CI, 1.017–2.125], $p = 0.040$), UVM (HR = 1.513 [95% CI, 1.068–2.144], $p = 0.020$), PAAD (HR = 1.576 [95% CI, 1.223–2.030], $p < 0.001$), and LGG (HR = 1.790 [95% CI, 1.391–2.304], $p < 0.001$). However, as illustrated in the image, the OS time in READ was extended with upregulation of TAP2 (HR = 0.519 [95% CI, 0.283–0.952], $p = 0.034$) (Fig. 3B). The four OS survival curves confirmed the results from the previous heat map. In the BLCA and OV tumor cohorts, OS improved with higher TAP2 expression, while the opposite trend was observed in LGG and ACC (Fig. 3C–F).

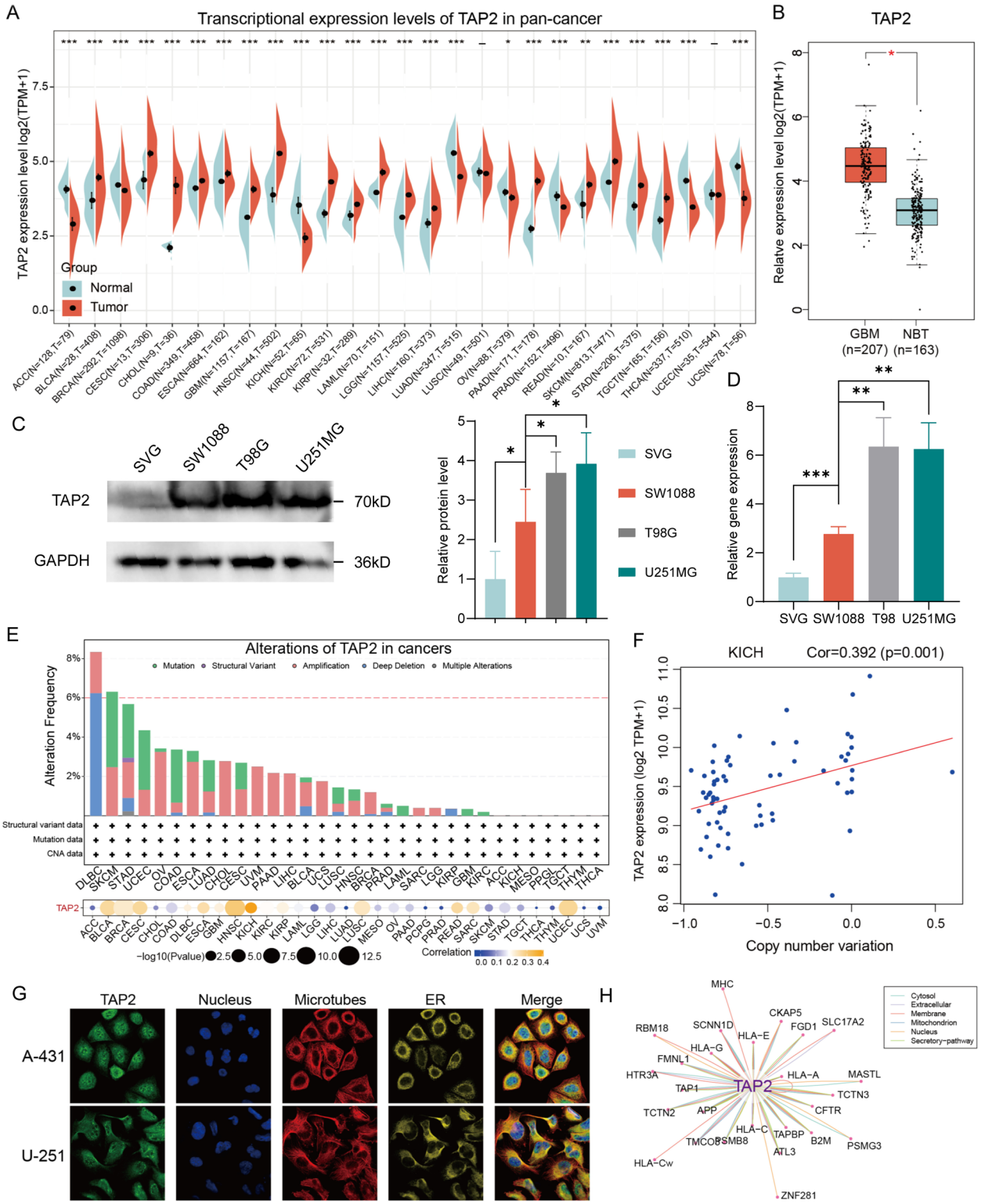

Fig. 2 The expression of TAP2 in human cancers. **A** Transcription expression level analysis of TAP2 between tumor and normal tissues by using the data from TCGA and GTEx databases. **B** The expression level of TAP2 between GBM and normal brain tissues. **C** The expression of TAP2 in different cell lines was analyzed by Western blot assay. **D** The expression of TAP2 in different cell lines was analyzed by RT-qPCR assay. **E** TAP2 alteration frequency analysis in pan-cancer by using the data from cBioPortal database. **F** The copy number variation of TAP2 in pan-cancer. **G** Immunofluorescence images and combination images of TAP2 protein, nucleus, microtubule, and endoplasmic reticulum (ER) in A-431 and U251 cell lines. (H) TAP2 interacting proteins are represented using protein–protein interaction (PPI) networks (*p < 0.05, **p < 0.01, ***p < 0.001)

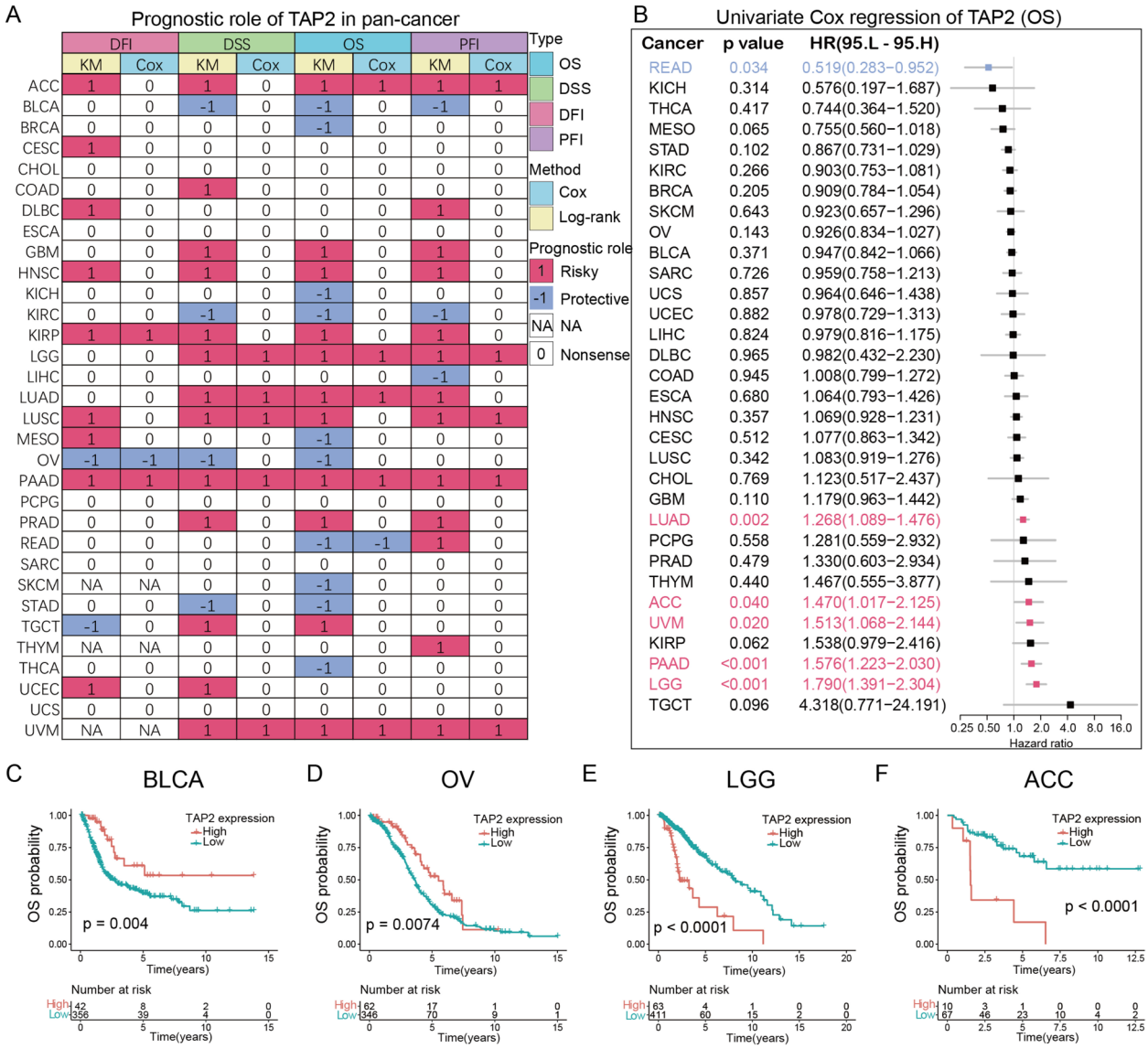

Fig. 3 Prognosis implication of TAP2 in human cancers. **A** Based on univariate Cox regression and Kaplan–Meier model, TAP2 expression was associated with overall survival (OS), disease-specific survival (DSS), disease-free interval (DFI), and progression-free interval (PFI). Red indicates that PDIA3 is a risk factor affecting the prognosis of cancer patients, while blue indicates a protective factor. Only results with P < 0.05 are shown. **B** Forest maps showing the prognostic effect of TAP2 in pan-cancer were prepared using univariate Cox regression method. Red indicates TAP2 is a statistically significant risk factor for prognosis, and blue indicates TAP2 is a protective factor. **C**–**F** Kaplan–Meier overall survival curves of TAP2 in BLCA (**C**), OV (**D**), LGG (**E**) and ACC (**F**)

Single cell expression of TAP2 in pan-cancer

The TISCH web tool was used to perform a single-cell analysis of TAP2 expression to identify the primary cell types expressing TAP2 in tumors, analyzing data from 79 single-cell cancer samples. According to the heatmap, TAP2 was primarily expressed in Endo and immune cells, particularly in monocytes/macrophages (Fig. 4A).

Gene set enrichment analysis of TAP2

To elucidate the hallmarks of TAP2-related tumors, GSEA was employed to identify DEGs between low-TAP2 and high-TAP2 subtypes across various tumors. Figure 5 illustrates the conclusion, which states that, in most tumors, multiple tumor-related and immune-related pathways were significantly activated in the TAP2 high-expression group. The pathways TNFA-signaling via NFKB, IFN-γ-response, IFN-α-response,

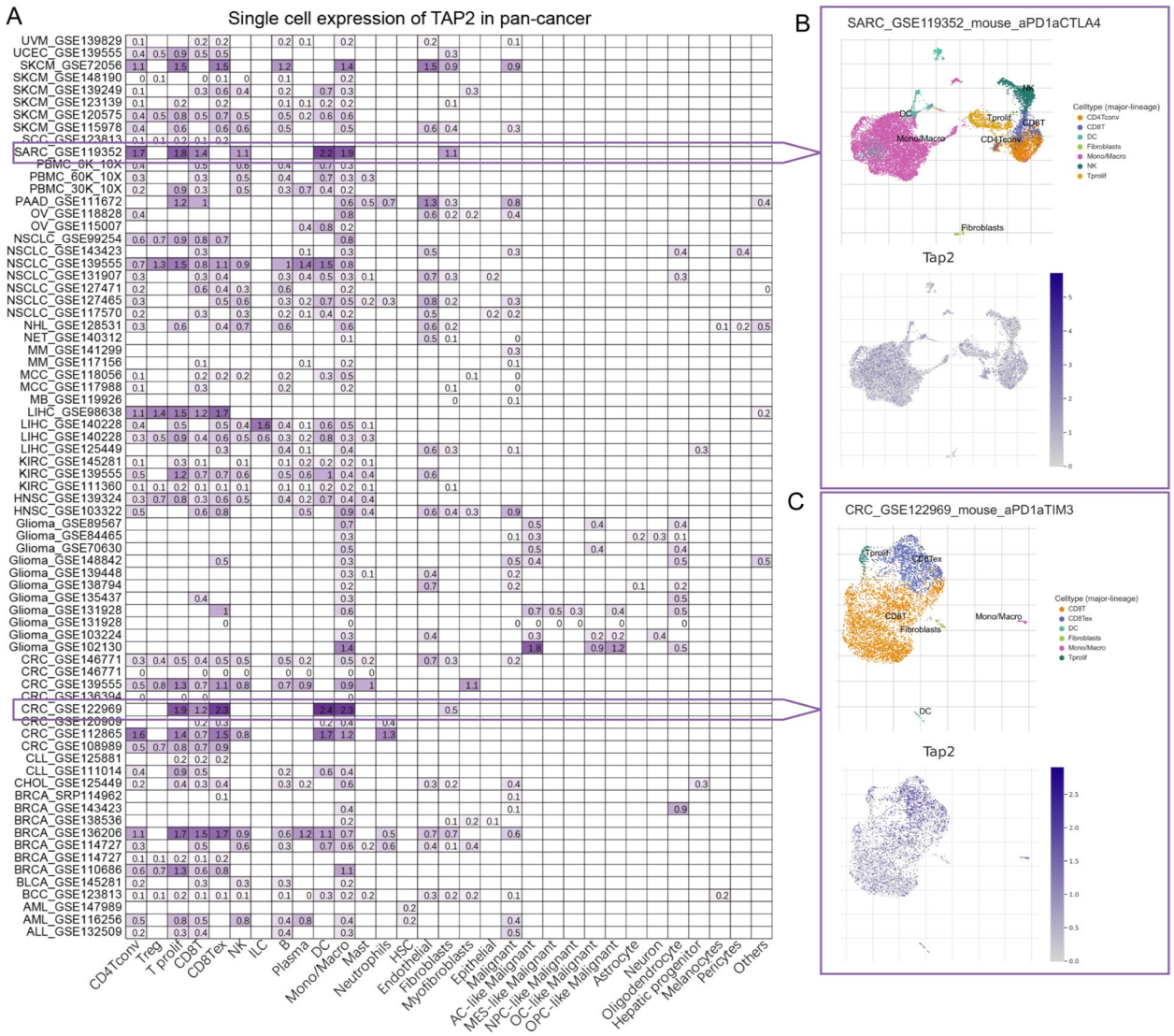

Fig. 4 Exploration for the expression of TAP2 at single-cell level. **A** TAP2 expression of 31 cell types in 73 single cell datasets. **B** Scatter plots showed the distribution of 7 cell types and the expression of TAP2 in different cell species in SARC_GSE119352 dataset. **C** Scatter plots showed the distribution of 6 cell types and the expression of TAP2 in different cell species in CRC_GSE122969 dataset

IL2-STAT5-signaling, IL6-JAK-STAT3-signaling, inflammatory-response, complement, allograft-rejection, and KRas signaling demonstrated a clear correlation with TAP2 expression across all 33 analyzed cancers. Additionally, apoptosis showed a significant correlation with TAP2 expression in CESC, GBM, KICH, LGG, OV, PAAD, SARC, SARC, and UCS. The results showed that TAP2 in the tumor microenvironment was associated with immune activation across various tumors. Furthermore, TAP2 appeared to influence tumor occurrence and progression through modulating immune pathways. The specific relationship and mechanisms of action between TAP2 and these pathways remain unclear; however, the findings offer valuable insights and directions for future research.

Immune cell infiltration analyses of TAP2

A positive correlation was observed between TAP2 and the infiltration levels of Treg, Tfh, Neutrophil, Monocyte, Macrophage, Dendritic cell, NK cell, CD8 + T cells, and B cell in nearly all tumor types. In contrast, TAP2 exhibited a negative correlation with the infiltration degree of HSC and MDSC (Fig. 6). Among these, macrophages warrant special attention. Although the infiltration of most cell types positively correlated with TAP2 expression, the M2-tide of macrophages

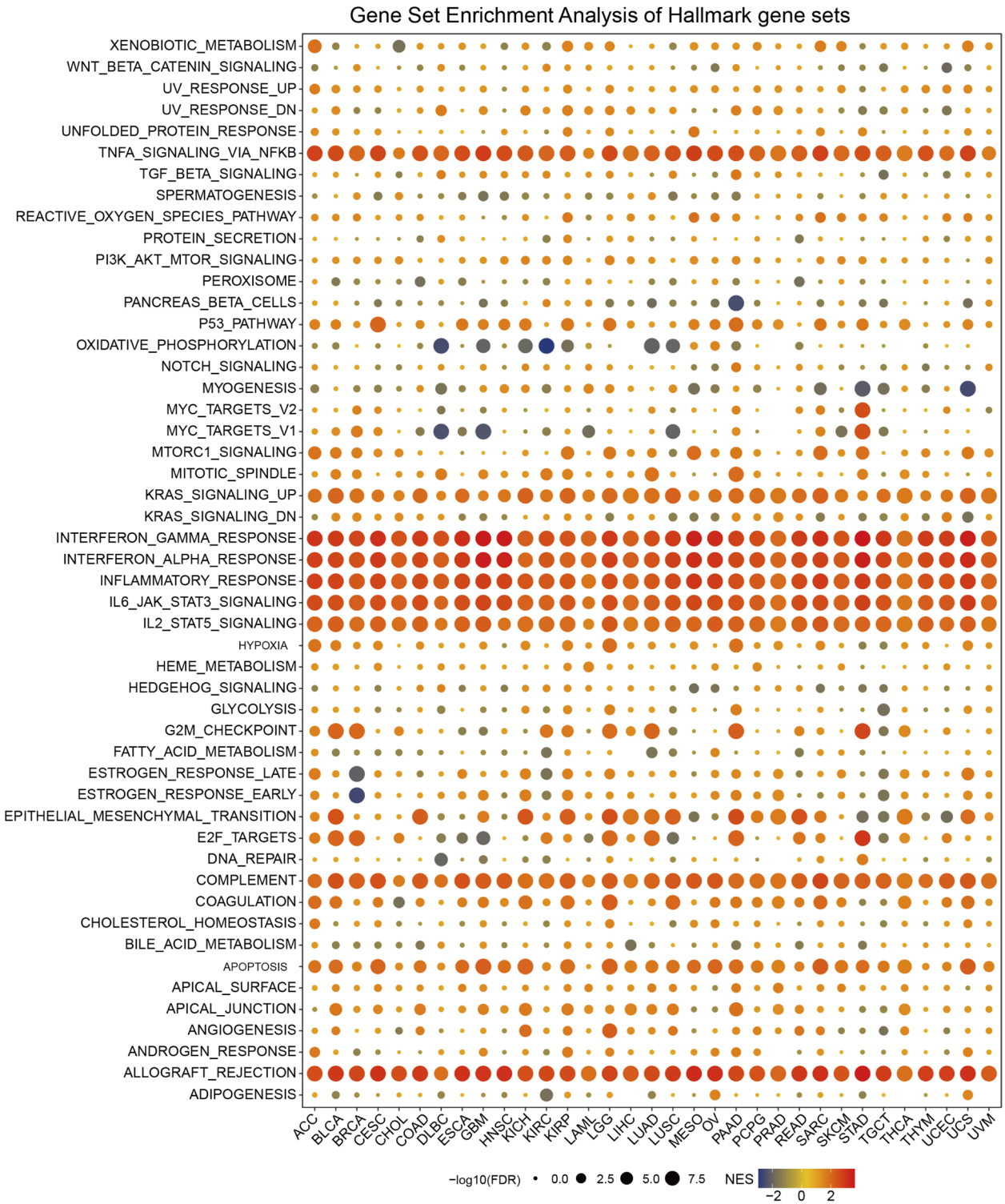

Fig. 5 The gene set enrichment analysis of TAP2 in pan-cancer. The color represents the normalized enrichment score (NES), and the size of the circles represents the FDR value of the enrichment items

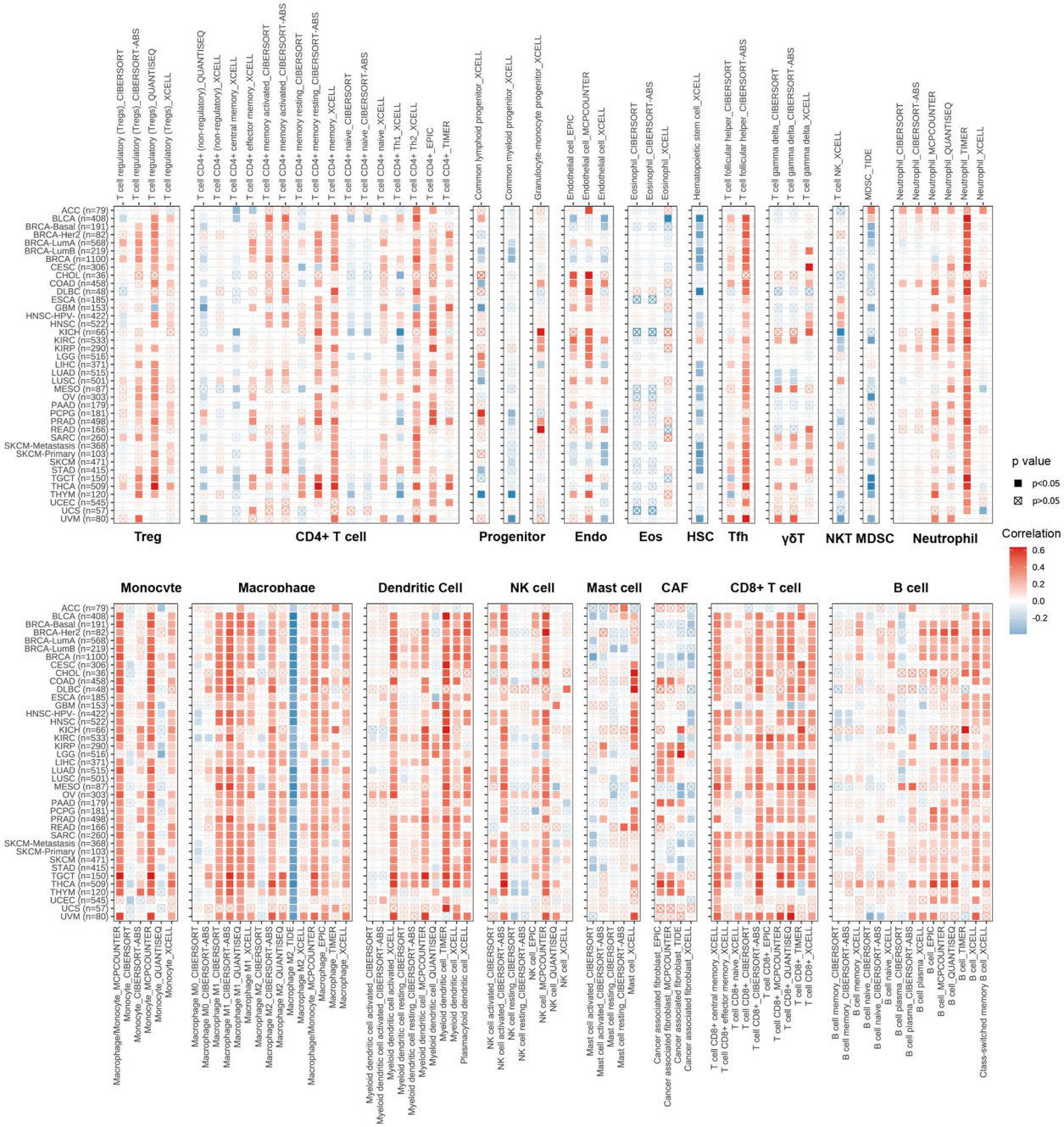

Fig. 6 Correlation analysis between TAP2 expression and immune cell infiltration. Red indicates a positive correlation and blue indicates a negative correlation

exhibited a negative correlation across all TCGA cancers. The cause of this abnormal result remains unclear; however, it may be related to the effect of TAP2 on the immune mechanism of the cancer. The specific role of TAP2 in the immunomodulatory effects across pan-cancer requires further investigation.

The predictive role of TAP2 in tumor immunotherapy

In pan-cancer, the relationship between TAP2 and 47 immune regulators was analyzed. The results showed that several immune regulators were positively correlated with TAP2 in most tumors, especially LAG3, ICOS, IDO1, TIGIT, and CD274 exhibited strong positive correlations across nearly all cancers. A few immune

regulators, such as VTCN1 and BTNL2, showed no significant association with TAP2 in most tumors (Fig. 7A). Combining TMB with MIS and TAP2 expression levels, multivariate Cox proportional hazards models were used to assess the effect of TAP2 on the response of patients to ICIs. A positive correlation was observed between TMB and UCS, BLCA, BRCA, CESC, COAD, LAML, LGG, LIHC, LUAD, SARC, SARC SKCM, STAD, and THCA, with no negative correlations identified between cancer types and TMB (Fig. 7B). BRCA, COAD, READ, and

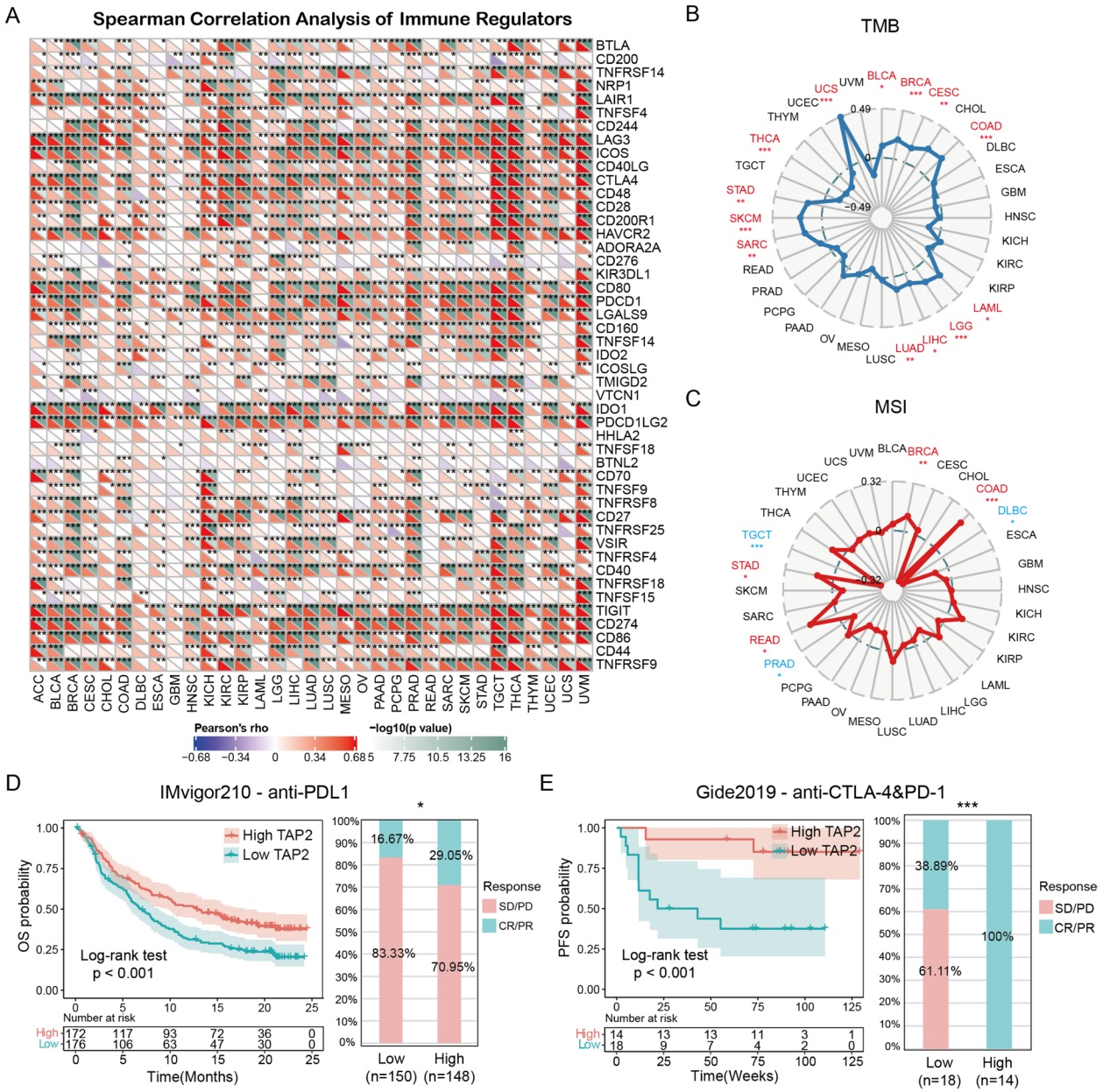

Fig. 7 TAP2 is associated with immune checkpoints and cancer immunotherapy response. **A** The spearman correlation heatmap depicts the correlations between the TAP2 expressions and immune regulators. Red represents positive correlation and blue represent negative correlation. **B** The correlation between TAP2 expression and TMB. Red represents positive correlation and blue represent negative correlation. **C** The correlation between TAP2 expression and MSI. Red represents positive correlation and blue represent negative correlation. **D** Kaplan–Meier curve of TAP2-expressing and high-expressing patients after anti-PDL1 treatment and Proportion of patients responding to anti-PDL1 treatment (IMvigor210 cohort). **E** Kaplan–Meier Graph of TAP2-expressing and high-expressing patients after anti-CTLA4 and PD-1 treatment versus Proportion of patients responding to anti-CTLA4 and PD-1 treatment (Gide2019 cohort). The labelled asterisk indicated the statistical p value (*p < 0.05, **p < 0.01, ***p < 0.001)

STAD exhibited positive correlations with MSI, while DLBC, PRAD, and TGCT showed negative correlations with MSI (Fig. 7C).

To further elucidate the predictive role of TAP2 in ICI immunotherapy for cancer, a statistical analysis was conducted to assess the relationship between TAP2 and ICI therapy response among patients with cancer. Figure 7D depicts that, among patients with urological tumors in the IMvigor210 cohort treated with anti-Programmed cell death 1 ligand 1(PDL1) therapy, those with high TAP2 expression exhibited longer OS and higher CR/PR response rate than those with low TAP2 expression. Similar results were observed in the Gide2019 cohort for melanoma, where patients with high TAP2 expression who underwent anti-cytotoxic T-lymphocyte-associated protein 4 (CTLA-4) and PDL1 therapy experienced significantly longer progression-free survival (PFS) than those with low expression. This result was particularly significant in response rates, as 100% of patients with melanoma with high TAP2 expression achieved complete or partial responses following anti-CTLA-4 and PDL1 treatment (Fig. 7E). These findings indicate that TAP2 plays a significant role in predicting the effectiveness of immunotherapy in tumors, providing valuable insights for the clinical treatment of patients with cancer.

High expression of TAP2 enhanced the migration and proliferation of glioma cells

To further elucidate the effect of TAP2 overexpression on the malignant biological behavior of glioma cells, a TAP2-overexpressing U251MG cell line was generated. Transwell, EdU labeling, wound healing, and clonal formation assays were performed to clarify the mechanisms through which TAP2 enhances the malignancy of glioma from various perspectives.

The TAP2-overexpressed plasmid was initially constructed, packaged with lentivirus, and transfected into U251MG cells. Western blotting was employed to detect changes in intracellular protein levels. The migration distance of cells overexpressing TAP2 was significantly greater than that of the control group during the same culture time after scribing (Fig. 8A and B). Similarly, TAP2 also enhanced the proliferation of GBM cells. In U251MG cells stained with EdU and Hoechst, the proportion of cells in the proliferative stage was higher in the experimental group than that in the control group (Fig. 8C and D). The same result was observed in the Transwell migration assay, where U251MG cells overexpressing TAP2 demonstrated a greater ability to traverse the bottom membrane than the control group. This finding further indicates that high expression of TAP2 may enhance the migration ability of tumor cells (Fig. 8E). The difference was statistically significant (Fig. 8F). However, although glioma cells with high TAP2 expression exhibited enhanced migration and proliferation, no significant difference was observed in clonogenesis ability between these glioma cells with high TAP2 expression and non-glioma cells (Fig. 8G and H). In conclusion, TAP2 overexpression enhances the migration and proliferation ability of glioma cells, potentially explaining its increased levels in high-grade gliomas.

TAP2 targeted small molecule drug screening in tumors

To investigate the potential of TAP2 as a target for tumor-directed therapy, small molecule inhibitors capable of targeting TAP2 across various tumors were screened. Our analysis revealed several agents with the ability to target pan-cancer. TG-101348 emerged as the most versatile, demonstrating efficacy in over 15 tumor types. Following closely were NU-7441, CAY-10618, ampicillin, and zosuquidar, which exhibited efficacy in more than 10 cancer types (Fig. 9A). The primary mechanisms of action of these drugs were further investigated. Figure 9B illustrates that these drugs primarily function as adrenergic receptor antagonists and EGFR inhibitors.

Subsequently, molecular docking technology was employed to conduct docking studies of several small molecule inhibitors that exhibited low binding energies to TAP2. This approach enabled us to visualize the detailed binding interactions between these small molecule inhibitors and TAP2. Significant findings include ampicillin (− 6.5 kcal/mol), TG-101348 (− 6.88 kcal/mol), and CAY-10618 (− 7.193 kcal/mol) (Fig. 9C–E).

Discussion

Studies show that tumor growth is closely linked to immune suppression [36–38]. Tumor cells activate various immune checkpoint pathways to promote immune suppression [39, 40]. Advancements in immunotherapy have led to significant breakthroughs in cancer treatment [41–43]. Currently, some cancers can be treated with precisely targeted therapies, such as those for EGFR-mutated NSCLC, which demonstrate considerable efficacy [44–46]. As a combination of immunotherapy and targeted therapy, immune-targeted therapy offers hope for long-term remission in patients with advanced cancers [47–49]. However, many tumors still lack effective targeted immune therapy methods, and patients with tumors exhibit varying responses to immunotherapy. Accurate prediction of patient response to immunotherapy is crucial for the clinical treatment of patients with cancer.

The role of TAP2 in immune function was investigated, and several cell function experiments were performed. Our findings indicate that TAP2 serves as a biomarker

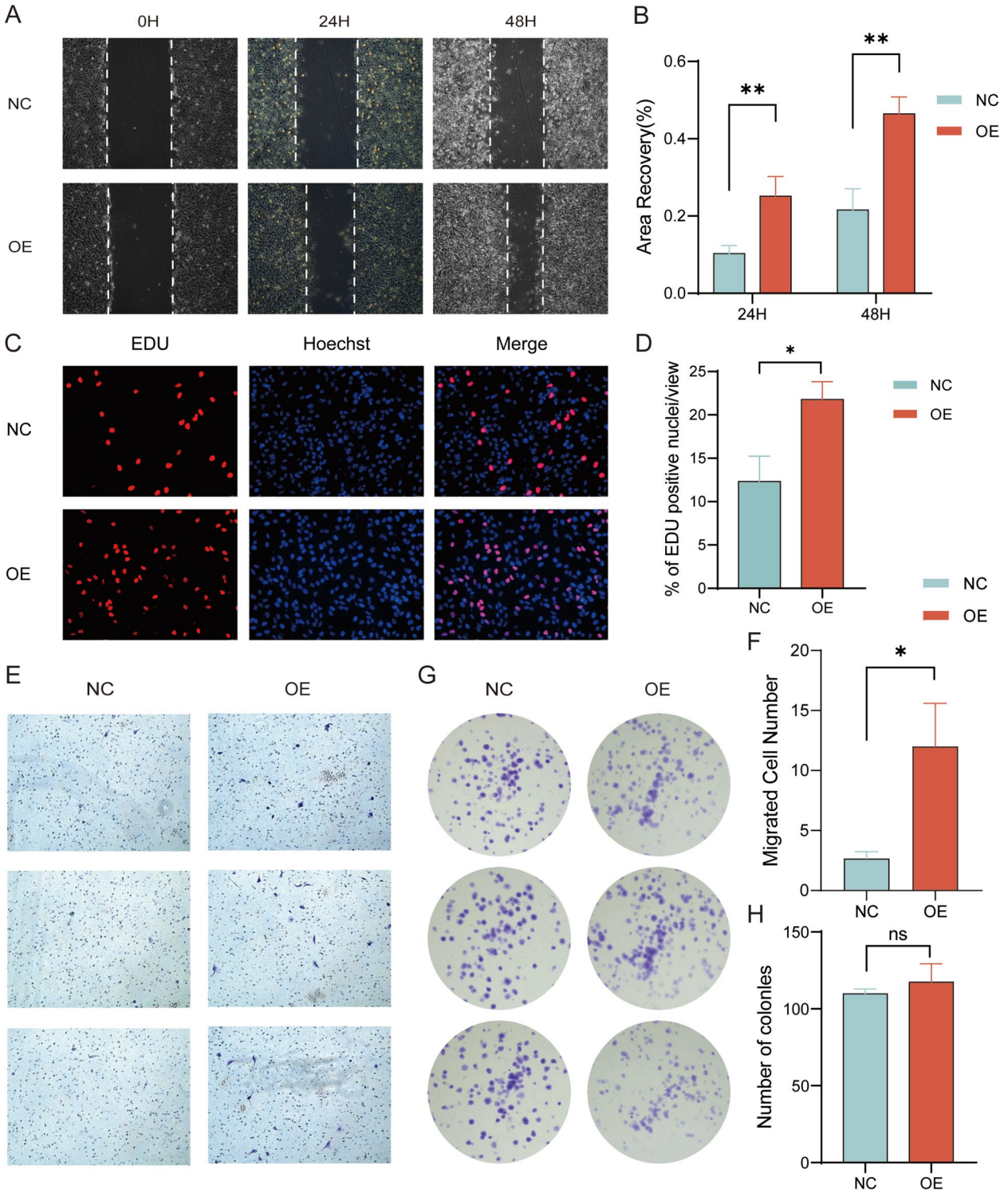

Fig. 8 Over-expression of TAP2 enhances malignant behavior of GBM cells. **A**, **B** The wound healing assay. **C**, **D** EdU cell proliferation assay. **E**, **F** The Transwell Migration Assay. **G**, **H** The Clonal Formation Experiment. NC indicated negative control and OE indicated over expression of TAP2. The labelled asterisk indicated the statistical p value (*$p < 0.05$, **$p < 0.01$, ***$p < 0.001$)

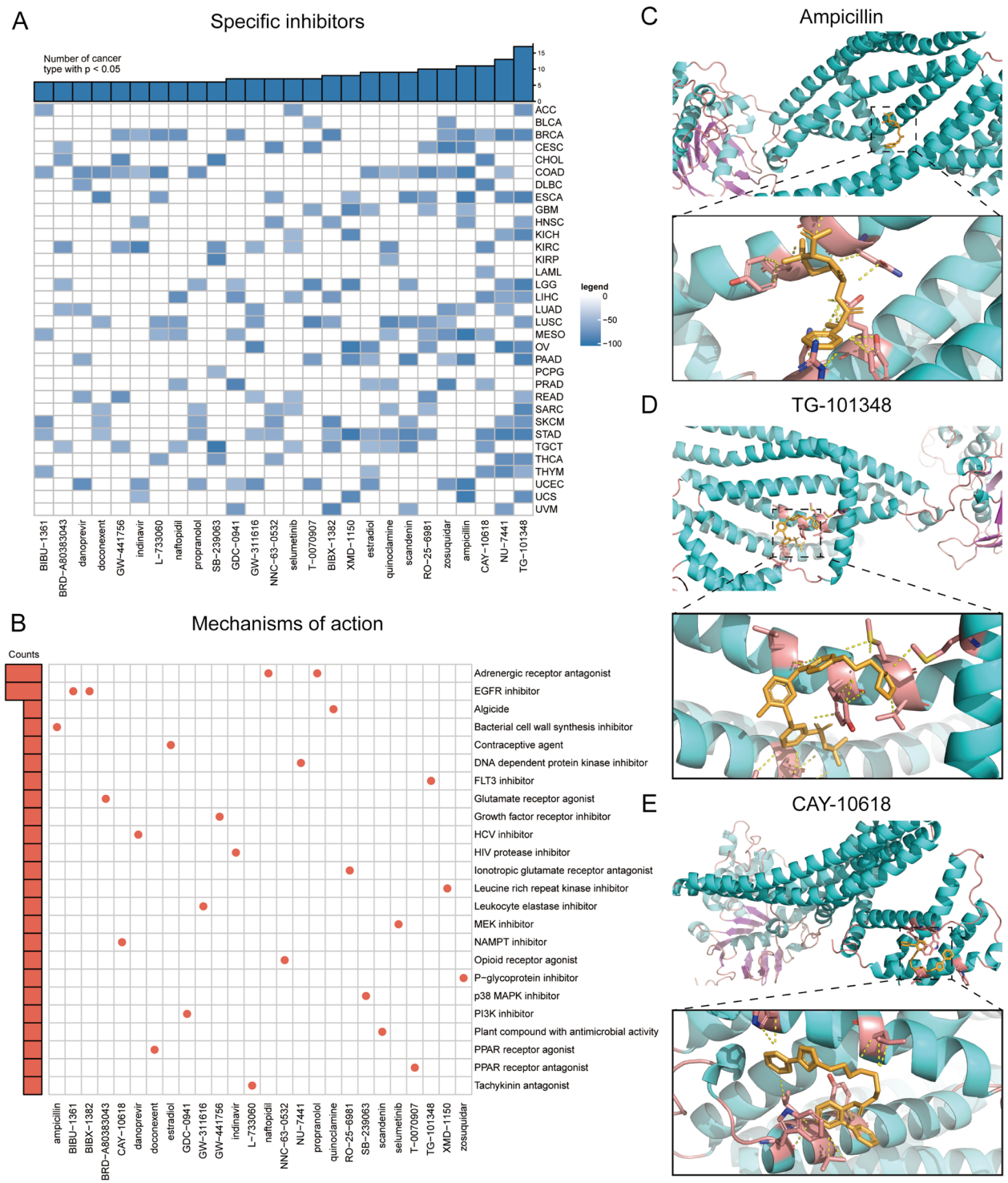

Fig. 9 Prediction analysis of small molecule drugs targeting TAP2 in pan-cancer. **A** The heatmap illustrates potential specific drugs targeting TAP2 enriched in more than 8 types of tumors. **B** The scatter plot delineates the mechanisms of action of specific inhibitors. **C**, **E** Molecular docking results of the TAP2 protein with 3 drugs

that accurately predicts the response of patients to immunotherapy, making it effective for assessing immunotherapy efficacy in patients with tumors. Moreover, TAP2 shows potential for further exploration in tumor immunity.

TAP2 expression levels were compared and analyzed using data from the TCGA and GTEx databases across various tumor cells and normal tissues. The results showed that TAP2 expression levels were elevated in more than half of TCGA tumors, especially in CHOL and GBM, compared to those in normal tissues. TAP2, as a component of TAP, presents high-affinity peptides to MHC-I, and its downregulation is associated with tumor immune escape [50]. However, in our analysis, we observed that TAP2 was highly expressed in most tumors. In this regard, Andrea et al. report a similar conclusion in their study on breast cancer [51]. We propose that this phenomenon results from a higher infiltration of immune cells in the tumor microenvironment of high-grade tumors, which secrete immune factors and enhance TAP2 expression.

The role of TAP2 in the prognosis of patients with cancer was evaluated. Our analysis revealed a high degree of consistency across OS, DSS, DFI, and PFI levels—TAP2 expression correlates with the patient prognosis across various cancers, and its high expression may indicate an increased risk of tumor recurrence. K–M survival curves for LGG and ACC also revealed a correlation between elevated TAP2 expression and poor prognosis, while patients with BLCA and OV showed the opposite trend. Clinical studies show a significant association between TAP2 expression levels and the clinicopathological grade in patients with breast cancer [51]. In triple-negative breast cancer, the downregulation of proteins in the MHC-Class I antigen presentation pathway, including TAP2, is associated with significantly reduced recurrence-free and overall survival periods in patients [52]. Similarly, in vitro experiments using tumor cell lines and clinical samples demonstrate that gene polymorphism of TAP2 is strongly associated with increased risk, grade, and poor overall survival in cervical cancer [53]. Combined with our previous analysis of TAP2 expression, this finding suggests that TAP2 holds strong potential as a prognostic marker for patients with cancer. TAP2 expression in tumor cells may serve as a prognostic tool for some patients with cancer in the future.

TAP2 expression significantly correlates with the activation of multiple immune pathways in GSEA results, especially the TNFA-via-NFKB, IL2-STAT5-signaling, IFNα-response, IFNγ -response, IL6-JAK-STAT3-signaling, allograft-rejection. Ruth Heise et al. report that interferon-α mediates TAP1 expression via the JAK-STAT pathway in melanoma [54]. This finding suggests that interferon-α similarly enhances TAP2 expression through the same pathway, a phenomenon likely common across pan-cancer. The results of our analysis support this conjecture and reveal that in addition to interferon-α, interferon-γ likely plays a similar role. This finding provides new insights for exploring the mechanism of tumor development and treatment.

Further analysis of the correlation between TAP2 and immune cell infiltration revealed a significant correlation between TAP2 and the levels of various immune cells—such as DC, CD8 + T cells, macrophages, monocytes, and NK cells. These findings suggest that TAP2 significantly influences the composition of the tumor microenvironment, serving as a crucial factor for assessing tumor progression and prognosis. Increasing immune suppressive cells, such as M2 macrophages, is a primary mechanism of tumor immune escape [55–57].

The previous analysis confirms the rationale for TAP2 as a prognostic marker for tumors. The relationship between TAP2 and immune regulatory factors through Spearman correlation was then analyzed. TAP2 showed a positive correlation with various immune regulators in most tumors—particularly LAG3, ICOS, IDO1, TIGIT, and CD274. Therefore, high TAP2 expression likely enhances the immune response in tumor cells, or increased infiltration of immune cells in the high-grade tumor cell microenvironment may promote TAP2 expression. The multivariate Cox proportional hazards models of TMB and MSI with TAP2 also confirm this inference. We observed that antigenicity increases with high TAP2 expression in various tumor cells. Previous similar analyses reveal that TAP2 may regulate immune cell infiltration and the immune response in TME. Additionally, the glioma prognosis model established based on eight genes, including TAP2, effectively stratifies patients with glioma by grades, highlighting the potential of TAP2 in immunotherapy and clinical prognosis prediction [58]. The specific mechanism by which TAP2 increases immune cell infiltration represents a valuable research direction that may provide insights into tumor immunotherapy and warrants future studies.

The following survival curve further demonstrates the prognostic significance of TAP2 in ICI cancer. In the IMvigor210 cohort of patients with urinary tumors undergoing anti-PDL1 treatment, those with high TAP2 expression experience longer OS than those with low TAP2 expression. Additionally, the CR/PR remission rates were higher in patients with low TAP2 expression. In the Melanoma cohort of Gide 2019, patients with high TAP2 expression who underwent anti-CTLA-4 and PDL1 treatment have longer PFS than those with low expression. These findings indicate that TAP2 possesses strong prognostic properties in cancers, accurately predicting

responses to immune checkpoint blockade. Tumors with high TAP2 expression demonstrate better efficacy using immune therapy.

We conducted functional experiments to validate our findings. We observed a significant increase in the migration and proliferation abilities of TAP2 overexpressed GBM cells, though clonogenicity remains affected. These findings strongly suggest that abnormal TAP2 expression likely promotes the malignant behavior of GBM cells. To clarify the therapeutic potential of TAP2 as a tumor target, inhibitor drugs that can effectively target it were screened. Our findings indicate the effectiveness of several TAP2-targeting inhibitors in various tumor types. Molecular docking techniques were then employed to further identify the potential binding sites of these inhibitors to TAP2.

Although this study shows the feasibility of TAP2 as a prognostic marker for cancer from various perspectives, some limitations exist. For example, sequencing data was obtained from an open database, which introduced systematic bias for analysis. Additionally, our functional experiments and expression difference analyses were only verified in glioma cell lines. Expanding the range of tumor cell lines would strengthen the evidence for our conclusions. We have not identified the specific reasons why high TAP2 expression correlates with immune channel activation, immune cell infiltration, and immune regulatory factors, necessitating further experimental exploration. New mechanisms likely underlying these phenomena offer new insights for cancer immunotherapy research. We propose that using TAP2 to predict cancer prognosis is completely feasible and offers significant clinical value.

Conclusions

In conclusion, this study, based on a comprehensive generalized cancer analysis, shows that TAP2 has the potential to serve as a potent prognostic marker and immune target for human cancers. This potential is associated with genomic changes, cancer prognosis, immune infiltration, and immunotherapy response.

Abbreviations

ABC	ATP binding cassette
ACC	Adrenocortical cancer
BLCA	Bladder cancer
BRCA	Breast cancer
CESC	Cervical cancer
CHOL	Bile duct cancer
CMap	Connectivity map
CNV	Copy number variations
CI	Confidence interval
COAD	Colon cancer
CR	Complete response
DEGs	Differential expression genes
DFI	Disease-free interval
DLBC	Diffuse large B-cell lymphoma
DSS	Disease-specific survival
ESCA	Esophageal cancer
ER	Endoplasmic reticulum
Endo	Endothelial cells
FPPP	FFPE pilot phase II
GSEA	Gene set enrichment analysis
GBM	Glioblastoma
HNSC	Head and neck cancer
HR	Hazard ratio
HSCs	Hematopoietic stem cells
ICI	Immune checkpoint inhibitor
KICH	Kidney chromophobe
KIRC	Kidney clear cell carcinoma
KIRP	Kidney papillary cell carcinoma
LAML	Acute myeloid leukemia
LGG	Lower grade glioma
LIHC	Liver cancer
LUAD	Lung adenocarcinoma
LUNG	Lung cancer
LUSC	Lung squamous cell carcinoma
MESO	Mesothelioma
MSI	Microsatellite instability
NK	Natural killer cell
OV	Ovarian cancer
OS	Overall survival
PAAD	Pancreatic cancer
PCPG	Pheochromocytoma and paraganglioma
PDL1	Anti-programmed cell death 1 ligand 1
PFI	Progression-free interval
PVDF	Polyvinylidene fluoride
PDB	Protein Data Bank
PPI	Interaction
PRAD	Prostate cancer
PR	Partial response
READ	Rectal cancer
SARC	Sarcoma
SDS	Sodium dodecyl sulfate
SKCM	Melanoma
STAD	Stomach cancer
TAP2	Transporter 2, ATP binding cassette subfamily B member
Tfh	Follicular helper
TISCH	Tumor immune single-cell hub
TMB	Tumor mutation burden
TGCT	Testicular cancer
THCA	Thyroid cancer
THYM	Thymoma
UCEC	Endometrioid cancer
UCS	Uterine carcinosarcoma
UVM	Ocular melanomas

Supplementary Information

The online version contains supplementary material available at https://doi.org/10.1186/s40001-025-02360-6.

Supplementary material 1.

Acknowledgements

We sincerely acknowledge the contributions from the TCGA project, GTEx project, and GEO project.

Author contributions

ZT, KH, and XZ designed this study and refined the article; LY, YS and JG performed cytological experiments, data collection and visualization, bioinformatics or statistical analysis, and manuscript writing. JL, CW, ZF and LH revised this study. All the co-authors have approved the final version of the manuscript.

Funding
The research project is supported by the National Natural Science Foundation of China (Grant no. 82172989, 82273068 and 82260524); Key Research and Development projects in Jiangxi (Grant no. 20212BBG73021); Jiangxi Training Program for academic and technical leaders of major disciplines—Young talents program (Grant no. 20212BCJ23023); Key project of Science and Technology Innovation of Health Commission (Grant no. 2023ZD003); Jiangxi Provincial Natural Science Foundation (Grant no. 20232BAB206101); Jiangxi Province Department of Education Science and technology research project, China (Grant no. GJJ210177). Project Fund of Jiangxi Provincial Health Commission (20204343, 202130873, 202210044).

Availability of data and materials
No datasets were generated or analysed during the current study.

Declarations

Ethics approval and consent to participate
Not applicable.

Consent for publication
Not applicable.

Competing interests
The authors declare no competing interests.

Author details
[1]The 2nd Affiliated Hospital, Jiangxi Medical College, Nanchang University, Nanchang 330006, Jiangxi, China. [2]Jiangxi Province Key Laboratory of Neurological Diseases, Nanchang 330006, Jiangxi, China. [3]JXHC Key Laboratory of Neurological Medicine, Nanchang 330006, Jiangxi, China. [4]Institute of Neuroscience, Jiangxi Medical College, Nanchang University, Nanchang 330006, Jiangxi, China. [5]HuanKui Academy, Jiangxi Medical College, Nanchang 330031, China. [6]The MOE Basic Research and Innovation Center for the Targeted Therapeutics of Solid Tumors, Jiangxi Medical College, Nanchang University, Nanchang 330006, Jiangxi, China.

Received: 8 June 2024 Accepted: 5 February 2025
Published online: 13 March 2025

References

1. Bray F, et al. Global cancer statistics 2022: GLOBOCAN estimates of incidence and mortality worldwide for 36 cancers in 185 countries. CA Cancer J Clin. 2024;74(3):229–63.
2. Fane M, Weeraratna AT. How the ageing microenvironment influences tumour progression. Nat Rev Cancer. 2020;20(2):89–106.
3. Zabransky DJ, Jaffee EM, Weeraratna AT. Shared genetic and epigenetic changes link aging and cancer. Trends Cell Biol. 2022;32(4):338–50.
4. Ullah A, et al. Biological significance of EphB4 expression in cancer. Curr Protein Pept Sci. 2024;25(3):244–55.
5. Riley RS, et al. Delivery technologies for cancer immunotherapy. Nat Rev Drug Discov. 2019;18(3):175–96.
6. Chuah S, Chew V. High-dimensional immune-profiling in cancer: implications for immunotherapy. J Immunother Cancer. 2020. https://doi.org/10.1136/jitc-2019-000363.
7. Ruiz de Galarreta M, et al. beta-Catenin activation promotes immune escape and resistance to anti-PD-1 therapy in hepatocellular carcinoma. Cancer Discov. 2019;9(8):1124–41.
8. Gomez S, et al. Combining epigenetic and immune therapy to overcome cancer resistance. Semin Cancer Biol. 2020;65:99–113.
9. Cerezo M, et al. The role of mRNA translational control in tumor immune escape and immunotherapy resistance. Cancer Res. 2021;81(22):5596–604.
10. Taylor BC, Balko JM. Mechanisms of MHC-I downregulation and role in immunotherapy response. Front Immunol. 2022;13: 844866.
11. He Y, et al. Gut microbial metabolites facilitate anticancer therapy efficacy by modulating cytotoxic CD8(+) T cell immunity. Cell Metab. 2021;33(5):988–10007.
12. Blees A, et al. Structure of the human MHC-I peptide-loading complex. Nature. 2017;551(7681):525–8.
13. Barbet G, et al. TAP dysfunction in dendritic cells enables noncanonical cross-presentation for T cell priming. Nat Immunol. 2021;22(4):497–509.
14. Vitale M, et al. HLA class I antigen and transporter associated with antigen processing (TAP1 and TAP2) down-regulation in high-grade primary breast carcinoma lesions. Cancer Res. 1998;58(4):737–42.
15. Liu W, et al. The association of TAP polymorphisms with non-small-cell lung cancer in the Han Chinese population. Hum Immunol. 2021;82(12):917–22.
16. Liu R, Ma Y, Chen X. Quantitative assessment of the association between TAP2 rs241447 polymorphism and cancer risk. J Cell Biochem. 2019;120(9):15867–73.
17. Cheng Z, et al. LMP2 and TAP2 impair tumor growth and metastasis by inhibiting Wnt/β-catenin signaling pathway and EMT in cervical cancer. BMC Cancer. 2023;23(1):1128.
18. Lapenna A, Omar I, Berger M. A novel spontaneous mutation in the TAP2 gene unravels its role in macrophage survival. Immunology. 2017;150(4):432–43.
19. Lage H, et al. Enhanced expression of human ABC-transporter tap is associated with cellular resistance to mitoxantrone. FEBS Lett. 2001;503(2–3):179–84.
20. Qian Y, et al. Genetic association between TAP1 and TAP2 polymorphisms and ankylosing spondylitis: a systematic review and meta-analysis. Inflamm Res. 2017;66(8):653–61.
21. Rezaieyazdi Z, et al. Correlations and influence of TAP2 genes polymorphisms and systemic lupus erythematosus propensity. Curr Rheumatol Rev. 2021;17(4):404–11.
22. Moins-Teisserenc H, et al. TAP2 gene polymorphism contributes to genetic susceptibility to multiple sclerosis. Hum Immunol. 1995;42(3):195–202.
23. Dai YH, et al. Radiosensitivity index emerges as a potential biomarker for combined radiotherapy and immunotherapy. NPJ Genom Med. 2021;6(1):40.
24. Tu Z, et al. Pan-cancer analysis: predictive role of TAP1 in cancer prognosis and response to immunotherapy. BMC Cancer. 2023;23(1):133.
25. Gao J, et al. Integrative analysis of complex cancer genomics and clinical profiles using the cBioPortal. Sci Signal. 2013;6(269):1.
26. Nusinow DP, et al. Quantitative proteomics of the cancer cell line encyclopedia. Cell. 2020;180(2):387-402.e16.
27. Veres DV, et al. ComPPI: a cellular compartment-specific database for protein-protein interaction network analysis. Nucleic Acids Res. 2015;43(Database issue):D485–93.
28. Yu G, et al. clusterProfiler: an R package for comparing biological themes among gene clusters. OMICS. 2012;16(5):284–7.
29. Li T, et al. TIMER20 for analysis of tumor-infiltrating immune cells. Nucleic Acids Res. 2020;48(1):W509-w514.
30. Su X, et al. DNMT3A promotes glioma growth and malignancy via TNF-α/NF-κB signaling pathway. Transl Cancer Res. 2024;13(4):1786–806.
31. Su J, et al. Identification of SSBP1 as a ferroptosis-related biomarker of glioblastoma based on a novel mitochondria-related gene risk model and in vitro experiments. J Transl Med. 2022;20(1):440.
32. Ullah A, et al. Sanguinarine attenuates lung cancer progression via oxidative stress-induced cell apoptosis. Curr Mol Pharmacol. 2024;17: e18761429269383.
33. Liu J, et al. Hypoxia induced ferritin light chain (FTL) promoted epithelia mesenchymal transition and chemoresistance of glioma. J Exp Clin Cancer Res. 2020;39(1):137.
34. Xu J, et al. Cullin-7 (CUL7) is overexpressed in glioma cells and promotes tumorigenesis via NF-κB activation. J Exp Clin Cancer Res. 2020;39(1):59.
35. Eberhardt J, et al. AutoDock Vina 1.2.0: new docking methods, expanded force field, and python bindings. J Chem Inf Model. 2021;61(8):3891–8.
36. Radoja S, et al. Mice bearing late-stage tumors have normal functional systemic T cell responses in vitro and in vivo. J Immunol. 2000;164(5):2619–28.
37. Dighe AS, et al. Enhanced in vivo growth and resistance to rejection of tumor cells expressing dominant negative IFN gamma receptors. Immunity. 1994;1(6):447–56.
38. Shankaran V, et al. IFNgamma and lymphocytes prevent primary tumour development and shape tumour immunogenicity. Nature. 2001;410(6832):1107–11.

39. Ding J, et al. Hedgehog signaling, a critical pathway governing the development and progression of hepatocellular carcinoma. Cells. 2021. https://doi.org/10.3390/cells10010123.
40. Darvin P, et al. Immune checkpoint inhibitors: recent progress and potential biomarkers. Exp Mol Med. 2018;50(12):1–11.
41. Herbst RS, et al. Atezolizumab for first-line treatment of PD-L1-selected patients with NSCLC. N Engl J Med. 2020;383(14):1328–39.
42. Schmid P, et al. Atezolizumab and Nab-Paclitaxel in advanced triple-negative breast cancer. N Engl J Med. 2018;379(22):2108–21.
43. Topalian SL, et al. Mechanism-driven biomarkers to guide immune checkpoint blockade in cancer therapy. Nat Rev Cancer. 2016;16(5):275–87.
44. Rosell R, et al. Erlotinib versus standard chemotherapy as first-line treatment for European patients with advanced EGFR mutation-positive non-small-cell lung cancer (EURTAC): a multicentre, open-label, randomised phase 3 trial. Lancet Oncol. 2012;13(3):239–46.
45. Ramalingam SS, et al. Overall survival with osimertinib in untreated, EGFR-mutated advanced NSCLC. N Engl J Med. 2020;382(1):41–50.
46. Wu YL, et al. Postoperative chemotherapy use and outcomes from ADAURA: osimertinib as adjuvant therapy for resected EGFR-mutated NSCLC. J Thorac Oncol. 2022;17(3):423–33.
47. Zou S, et al. Targeting STAT3 in cancer immunotherapy. Mol Cancer. 2020;19(1):145.
48. Lam TC, et al. Combination atezolizumab, bevacizumab, pemetrexed and carboplatin for metastatic EGFR mutated NSCLC after TKI failure. Lung Cancer. 2021;159:18–26.
49. Hack SP, et al. IMbrave 050: a Phase III trial of atezolizumab plus bevacizumab in high-risk hepatocellular carcinoma after curative resection or ablation. Future Oncol. 2020;16(15):975–89.
50. Lankat-Buttgereit B, Tampe R. The transporter associated with antigen processing: function and implications in human diseases. Physiol Rev. 2002;82(1):187–204.
51. Henle AM, et al. Downregulation of TAP1 and TAP2 in early stage breast cancer. PLoS ONE. 2017;12(11): e0187323.
52. Pedersen MH, et al. Downregulation of antigen presentation-associated pathway proteins is linked to poor outcome in triple-negative breast cancer patient tumors. Oncoimmunology. 2017;6(5): e1305531.
53. Gostout BS, et al. TAP1, TAP2, and HLA-DR2 alleles are predictors of cervical cancer risk. Gynecol Oncol. 2003;88(3):326–32.
54. Heise R, et al. Interferon alpha signalling and its relevance for the upregulatory effect of transporter proteins associated with antigen processing (TAP) in patients with malignant melanoma. PLoS ONE. 2016;11(1): e0146325.
55. Ye Y, et al. Long non-coding RNA cox-2 prevents immune evasion and metastasis of hepatocellular carcinoma by altering M1/M2 macrophage polarization. J Cell Biochem. 2018;119(3):2951–63.
56. Boutilier AJ, Elsawa SF. Macrophage polarization states in the tumor microenvironment. Int J Mol Sci. 2021. https://doi.org/10.3390/ijms22136995.
57. Zhao C, et al. Nanomaterials targeting tumor associated macrophages for cancer immunotherapy. J Control Release. 2022;341:272–84.
58. Su J, et al. Identification of a tumor microenvironment-related eight-gene signature for predicting prognosis in lower-grade gliomas. Front Genet. 2019;10:1143.

Publisher's Note